iScience

CellPress
OPEN ACCESS

Article

Amiloride reduces fructosamine-3-kinase expression to restore sunitinib sensitivity in renal cell carcinoma

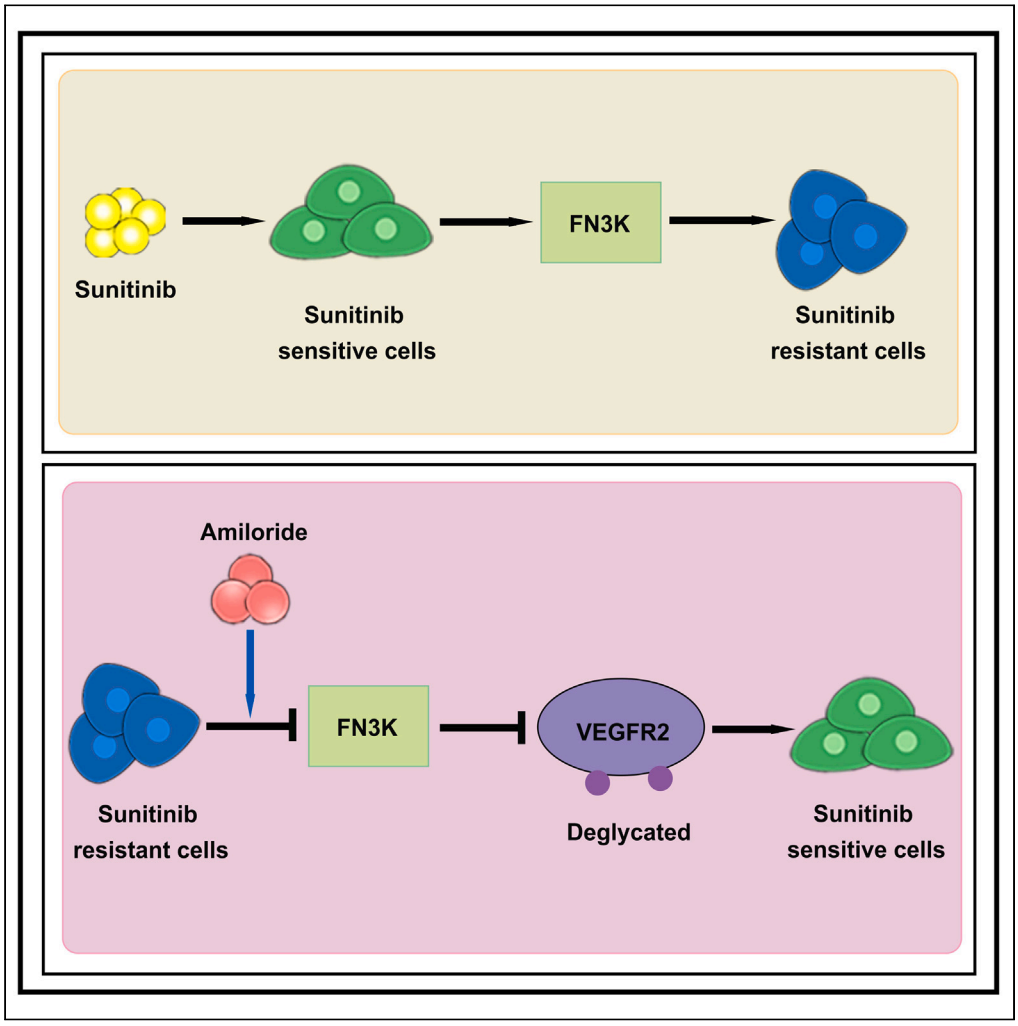

Yuanyuan Bai, Yiqing You, Daoxun Chen, ..., Yingming Sun, Lixian Wu, Yongyang Wu

yingmingsun@fjmu.edu.cn (Y.S.)
wlx-lisa@fjmu.edu.cn (L.W.)
wuyyfj@fjmu.edu.cn (Y.W.)

Highlights

Amiloride has anti-tumor activity in renal cell carcinoma

We identified the anti-tumor effect of Amiloride in conjunction with Sunitinib in renal cell carcinoma, along with its safety profile

FN3K involved in Amiloride synergizing the anti-RCC activity of sunitinib

FN3K induced Sunitinib resistance in RCC by affecting VEGFR2 expression

Bai et al., iScience 27, 109997
June 21, 2024
https://doi.org/10.1016/j.isci.2024.109997

iScience

CellPress
OPEN ACCESS

Article

Amiloride reduces fructosamine-3-kinase expression to restore sunitinib sensitivity in renal cell carcinoma

Yuanyuan Bai,[1] Yiqing You,[2] Daoxun Chen,[1] Yongmei Chen,[1] Zhenjie Yin,[1] Shangfan Liao,[1] Bingyong You,[1] Dongming Lu,[1] Yingming Sun,[3,*] Lixian Wu,[4,5,*] and Yongyang Wu[1,6,*]

SUMMARY

The kidney is a vital organ responsible for water and sodium metabolism, while the primary function of amiloride is to promote the excretion of water and sodium. We investigated amiloride enhanced the sunitinib sensitivity in RCC. We found both sunitinib and amiloride displayed cytotoxicity and exerted the synergy effect in RCC cells *in vivo* and *in vitro* arrays. Protein expression profiles were screened via MS/TMT, revealing that FN3K was upregulated in the sunitinib group, and rescued in amiloride and the combination administration. Exogenous FN3K could promote proliferation, invasion and metastasis and decrease the sensitivity of Caki-1 cells to sunitinib, also, exogenous FN3K up-regulated VEGFR2 expression and activated AKT/mTOR signal pathway. More FN3K and VEGFR2 accumulated in R-Caki-1 cells and rescued by amiloride treatment. Co-IP and IF confirmed the interaction between FN3K and VEGFR2. In conclusion, FN3K depletion mediated VEGFR2 disruption promotes amiloride synergized the anti-RCC activity of sunitinib.

INTRODUCTION

Renal cell carcinoma (RCC) originates in the urinary tubular epithelial system of the renal parenchyma and accounts for approximately 2%–3% of adult malignancies.[1,2] sunitinib is a first-line therapeutic agent for patients with intermediate and advanced RCC.[3] Although sunitinib is effective in improving overall survival (OS) and progression-free survival (PFS) in patients with advanced RCC, approximately 30% of patients are inherently resistant to sunitinib, with the remaining patients developing resistance around 6–15 months of treatment.[4,5] The main process of sunitinib resistance is angiogenesis in tumor microenvironment.[6] However, no drugs effectively counteract sunitinib resistance in RCC within clinical practice. Therefore, finding drugs that can restore sunitinib sensitivity and studying its underlying mechanism is essential in RCC.

ENaC is accountable for the absorption of Na^+ and the transportation of fluids, preserving homeostasis, and is significantly linked to the prognosis of RCC.[7,8] Our team previously found that ENaCs showed an oncogene profile in RCC and was an ideal biomarker for predicting the prognosis of RCC. Therefore, drugs targeting epithelial sodium channel may be a possible therapeutic way to treat RCC.[7] Amiloride, as an inhibitor targeting ENaC, can inhibit the growth of prostate and breast cancer in mice xenograft models in a dose-dependent manner.[9,10] Another study confirmed that amiloride could reduce the invasive capacity of human breast cancer cells by a basement membrane stromal invasion assay and inhibit tumor metastasis *in vivo*.[11] Recent studies have found amiloride completely inhibited the formation of capillary morphology and reduced neovascularization by 55% after amiloride treatment *in vivo* model of rabbit corneal angiogenesis.[12] Notably, VEGF mRNA levels were significantly reduced when amiloride was applied to treat leukemic cells.[13] In conclusion, amiloride may have the potential to enhance the cancer-suppressive effects of sunitinib in RCC.

We sought to investigate the efficacy and safety of amiloride in conjunction with sunitinib, as well as to elucidate the molecular mechanism by which amiloride enhances sunitinib sensitivity in RCC.

RESULTS

Amiloride enhanced sunitinib sensitivity in renal cell carcinoma cell lines

Caki-1 and 786-O cells were subjected to co-incubation with varying concentrations of sunitinib and amiloride. The inhibitory effects of both sunitinib and amiloride on RCC cells were found to be concentration-dependent, with amiloride significantly enhancing the cytotoxicity of

[1]Department of Urology, Affiliated Sanming First Hospital, Fujian Medical University, Sanming, Fujian 365100, P.R. China
[2]Key Laboratory of Diagnostic Medicine Designated by the Chinese Ministry of Education, Chongqing Medical University, Chongqing 400016, China
[3]Department of Oncology, Affiliated Sanming First Hospital, Fujian Medical University, Sanming, Fujian 365100, P.R. China
[4]Department of Pharmacology, School of Pharmacy, Fujian Medical University, Fuzhou, China
[5]Fujian Key Laboratory of Natural Medicine Pharmacology, Fujian Medical University, Fuzhou, China
[6]Lead contact
*Correspondence: yingmingsun@fjmu.edu.cn (Y.S.), wlx-lisa@fjmu.edu.cn (L.W.), wuyyfj@fjmu.edu.cn (Y.W.)
https://doi.org/10.1016/j.isci.2024.109997

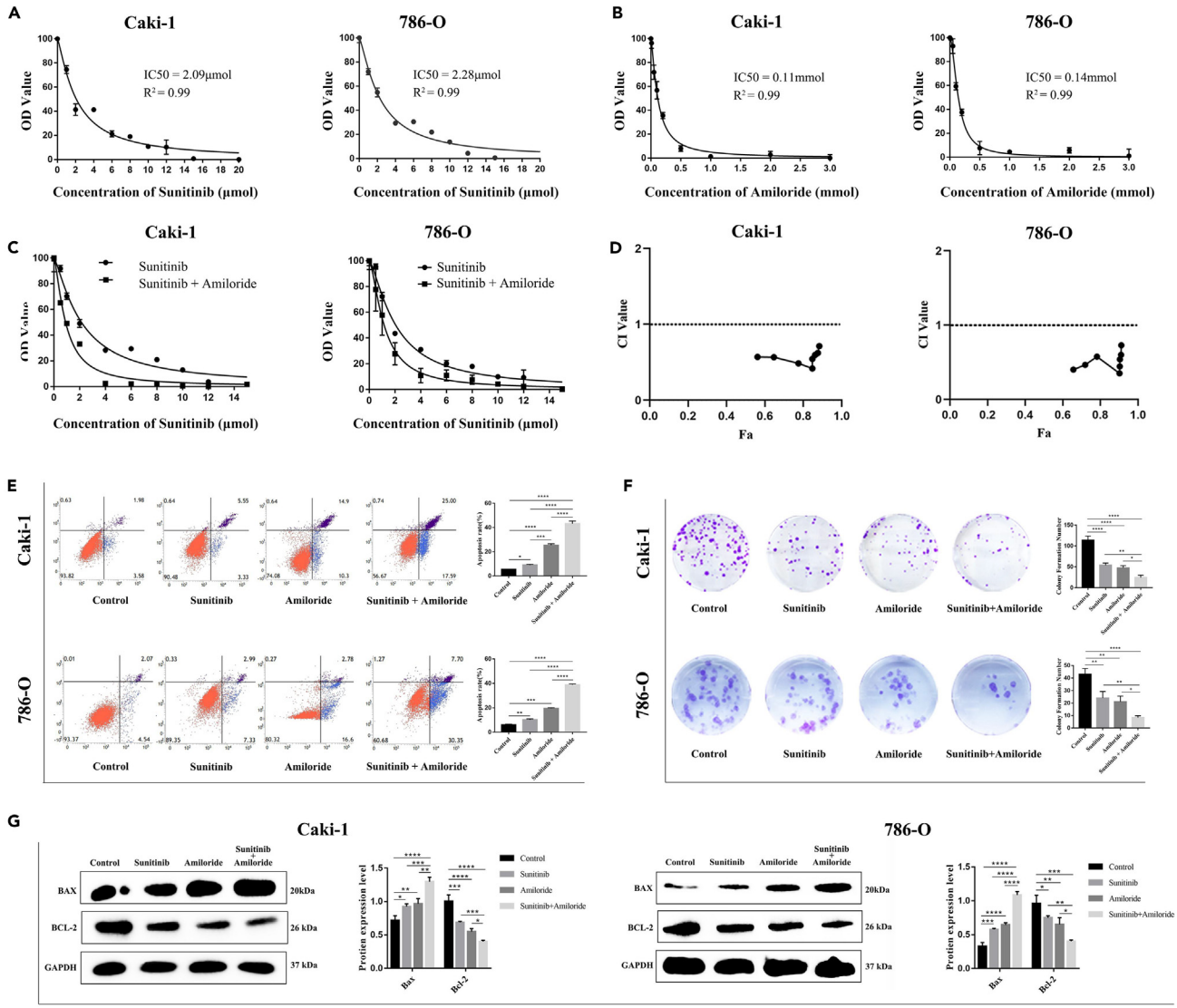

Figure 1. Amiloride enhanced the sunitinib sensitivity of RCC cells

(A and B) Caki-1 and 786-O cells were subjected to varying doses of sunitinib and amiloride, and their proliferation activity was assessed using the CCK-8 reagent.

(C) Caki-1 and 786-O cells were treated with different doses of sunitinib combined with 0.15mmol amiloride, and the proliferation activity of cells was detected by CCK-8 reagent.

(D) CI of different doses of sunitinib combined with 0.15mmol amiloride for 48h in Caki-1 and 786-O cells (Fa = Inhibition ratio).

(E) Caki-1 and 786-O cells were treated with 2μmol sunitinib, 0.15mmol amiloride and the combination of the two drugs for 48 h, and the apoptosis was detected by flow cytometry.

(F) Caki-1 and 786-O cells were treated with 2μmol sunitinib, 0.15mmol amiloride and the combination of the two drugs for 14 days to detect the ability of colony formation.

(G) The expression of apoptosis-related proteins Bcl-2 and Bax were evaluated through WB after 48h treatment with 2μmol sunitinib, 0.15mmol amiloride, and a combination of both drugs in Caki-1 and 786-O cells. *$p < 0.05$, **$p < 0.01$, ***$p < 0.001$, ****$p < 0.0001$.

sunitinib (Figures 1A–1C). Calculated by Kim's formula, the Q values of RCC cells treated with different concentrations of sunitinib and 0.15mmol amiloride were all more than 0.85 (Table 1). According to the calculation of CompuSyn software, the CI values of RCC cells treated with various doses of sunitinib and 0.15mmol amiloride were all less than 1 (Figure 1D). The above results showed that sunitinib combined with amiloride has a synergistic anti-proliferation effect on RCC cells. The results of the flow cytometry analysis revealed that the co-administration of sunitinib and amiloride elicited a greater induction of apoptosis compared to their individual treatment (Figure 1E). The colony formation assay revealed that both sunitinib and amiloride significantly impeded colony formation on the 14th day, and the combined treatment exhibited a synergistic effect (Figure 1F). Furthermore, WB analysis demonstrated the upregulation of BAX expression and downregulation

Table 1. Efficiency index of sunitinib combined with 0.15 mmol amiloride on RCC cells

	Sunitinib(μmol)							
Efficiency index (Q)	1	2	4	6	8	10	12	15
Caki-1	2.30	1.05	1. 16	1.01	0.93	0.91	0.93	0.91
786-O	2.56	1.63	1.03	1. 11	0.98	0.95	0.94	0.93

in Bcl-2 expression in the combination regimen of Sunitinib and amiloride, suggesting amiloride exerted the synergistic effect in combination with sunitinib on the activation of the apoptosis pathway (Figure 1G).

Amiloride augmented the response of renal cell carcinoma to sunitinib through fructosamine-3-kinase

We employed TMT-labeled quantitative proteomics to examine the protein expression profiles of Caki-1 cells in various drug-treated groups in order to identify potential key features of the anti-tumor effects of amiloride and sunitinib. Our findings revealed that sunitinib treatment up-regulated 62 proteins, whereas amiloride treatment down-regulated 97 proteins (Figure 2A). The overlapping of two datasets represented in the Venn diagram showed that FN3K down-regulation may be attributed to the epigenetic regulation of amiloride interference, which could enhance the therapeutic response of RCC to sunitinib (Figure 2B). Then, we further analyzed proteomics data from each group with FN3K levels (Figure 2C). Subsequently, FN3K expression was detected in Caki-1 cells, and treatment with sunitinib resulted in a significant increase in FN3K levels. This effect was effectively alleviated by amiloride, consistent with proteomic analysis (Figure 2D). Additionally, we analyzed RNA-sequencing expression profiles from patients with RCC in the TCGA cohort to confirm the underlying function of FN3K. Volcano maps and heat maps demonstrated differential genes associated with FN3K, while enrichment analysis revealed a potential relationship between FN3K with glycolysis and sodium ion transport in RCC (Figures 2E–2G).

Fructosamine-3-kinase overexpression promoted Caki-1 cell proliferation, migration, and invasion

In the TCGA database, we found that FN3K was associated with improved prognosis of RCC (Figures S1A and S1B). Patients with low-FN3K expression showed poor clinical stage and grade (Figures S1C–S1H). In addition, univariate Cox and multivariate COX regression analysis indicated that FN3K could be used as an independent prognostic factor for RCC (Figure S1I). Furthermore, we used FN3K expression abundance combined with clinical information to draw a nomogram map to identify the prognostic risk of patients with RCC (Figure S1J). Lentiviruses carrying FN3K overexpression were utilized to obtain Caki-1 cells with FN3K overexpression (Figure 2H). CCK-8 detection revealed that FN3K overexpression significantly stimulated cell proliferation (Figure 2I). The migratory capacity of Caki-1 cells was assessed via wound healing and transwell migration assays, which demonstrated that FN3K overexpression enhanced cell migration (Figures 2J–2L).

Fructosamine-3-kinase drives VEGFR2 expression to reduce sunitinib sensitivity in renal cell carcinoma

To evaluate the effect of FN3K on the anti-RCC response to sunitinib, we based on the TCGA dataset and the Genomics of Drug Sensitivity in Cancer (GDSC), we predict the correlation between FN3K and IC50 values of sunitinib. Our finding indicated a positive correlation between the expression of FN3K and the IC50 value of sunitinib in RCC (Figure 3A). As expected, drug sensitivity tests revealed that FN3K has the potential to elevate the IC50 of sunitinib in Caki-1 cells, thus implying that FN3K may impede the sensitivity of RCC to sunitinib (Figure 3B). The cultivation of drug-resistant strains serves as a valuable *in vitro* approach to investigate the mechanism of drug resistance in tumors, and has been extensively employed in prior research. In this study, we cultured Caki-1 cell lines that were resistant to sunitinib to further examine the underlying mechanism (RI > 5, R-Caki-1) (Figure 3C). WB analysis revealed that FN3K was elevated in S-Caki-1 cells (treatment with sunitinib for 48 h) whereas VEGFR2, which is the primary target protein of sunitinib, was diminished, but both FN3K and VEGFR2 were up-regulated in R-Caki-1 cells (Figure 3D). Notably, we observed an upregulation of VEGFR2 when FN3K overexpressed in Caki-1 and 786-O cells (Figure 3E). It is postulated that a protein-protein interaction (PPI) may exist between FN3K, a de-glycating kinase, and the glycated receptor VEGFR2. To further validate this hypothesis, co-immunoprecipitation (Co-IP) was conducted in Caki-1 and 786-O cells to confirm the physical interaction between FN3K and VEGFR2 (Figure 3F). The FN3K and VEGFR2 laser scatterplots were linearly formed in Caki-1 and 786-O cells, which showed that FN3K and VEGFR2 co-localized (Figure 3G). VEGFR2 was purified by immunoprecipitation (IP), and it was observed that the molecular weight of VEGFR2 decreased following the overexpression of FN3K in Caki-1 cells, indicating that FN3K may facilitate the deglycation of VEGFR2 (Figure 3H). we detected the AKT/mTOR signal pathway of RCC cells after FN3K overexpression. The results showed that FN3K could stimulate the phosphorylation of AKT and mTOR (Figure 3I), indicating that FN3K mediates VEGFR2 enrichment and activates the AKT/mTOR signal pathway. Utilizing AutoDock Vina 1.1.2 docking analysis, it was determined that amiloride exhibited direct molecular docking with FN3K (Figure 3J). Furthermore, the application of amiloride to R-Caki-1 cells for a duration of 48 h resulted in the down-regulation of both FN3K and VEGFR2 expression levels. Furthermore, the application of amiloride to R-Caki-1 cells for a duration of 48 h, we observed that the proliferative activity of cells decreased and both FN3K and VEGFR2 were down-regulated (Figures 3K and 3L).

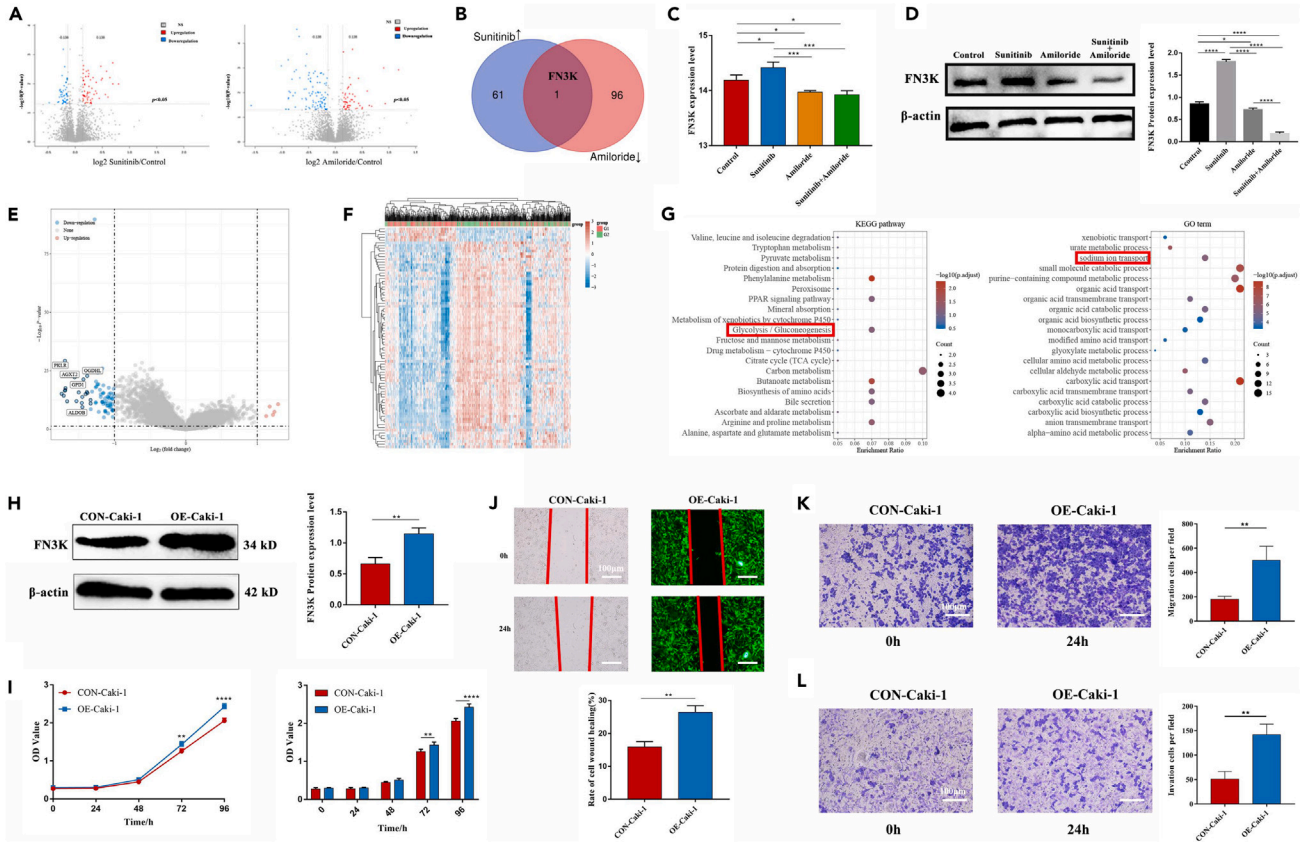

Figure 2. FN3K is a significant protein in amiloride to enhance the sensitivity of sunitinib to RCC

(A) Caki-1 cells were treated with 2μmol sunitinib, 0.15mmol amiloride and a combination of both drugs for 48h. The intracellular protein expression changes in each group were analyzed using labeled quantitative proteomics. Differential protein volcano maps of sunitinib and amiloride were generated in comparison to the control group.

(B) The Venn diagram illustrates FN3K was the hub protein in the synergistic action of amiloride (down-regulated protein, red) with sunitinib (up-regulated protein, blue).

(C and D) Caki-1 cells were subjected to treatment with 2μmol sunitinib, 0.15mmol amiloride, and a combination of both drugs for 48 h, followed by the detection of FN3K expression through proteomics and WB.

(E and F) The volcano plot and heatmap depict the differential gene expression profiles associated with FN3K, respectively.

(G) The GO and KEGG enrichment analyses were performed on genes related to FN3K.

(H) FN3K was successfully overexpressed in Caki-1 cells.

(I) The effect of FN3K on the proliferation of Caki-1 cells was evaluated using CCK-8 assay.

(J) The effect of FN3K on the migration of Caki-1 cells was detected by scratch test.

(K and L) Transwell chamber to detect the effect of FN3K on the migration and invasion of Caki-1 cells. $*p < 0.05$, $**p < 0.01$, $***p < 0.001$, $****p < 0.0001$.

Amiloride enhanced the anti-tumor effect of sunitinib *in vivo*

To investigate the *in vivo* anti-tumor effect of amiloride in combination with sunitinib, Caki-1 cells were introduced into the right axilla of BALB-c/Null mice. After ten days, when the tumor size reached approximately 150 mm^3, the mice were randomly assigned to four groups and administered different drugs to monitor tumor growth (Figure 4A). The combined treatment of amiloride and sunitinib demonstrated a significant inhibition of tumor volume and weight, exhibiting a synergistic effect. Compared with monotherapy, the combination therapy resulted in a more significant inhibition of tumor growth, which was quantified by tumor growth curve and tumor weight (Figures 4B–4D). The HE-stained tissue specimens of heart, liver, lung and kidney from mice did not show apparent toxic damage (Figure 4E). The results of the Ki-67 staining indicated that both sunitinib and amiloride independently hindered cell proliferation, and their combined administration produced a synergistic effect *in vivo* (Figure 5A). Additionally, TUNEL test demonstrated that the apoptotic potential of the combined therapy was more pronounced than that of either treatment alone (Figure 5B). Furthermore, the immunohistochemical findings of tumor sections indicated that FN3K was elevated in the sunitinib group, whereas it was reduced in the amiloride and combined groups, aligning with the outcomes of proteomics and WB analyses (Figure 5C). Additionally, VEGFR2 exhibited a decrease in response to various drug treatments (Figure 5D).

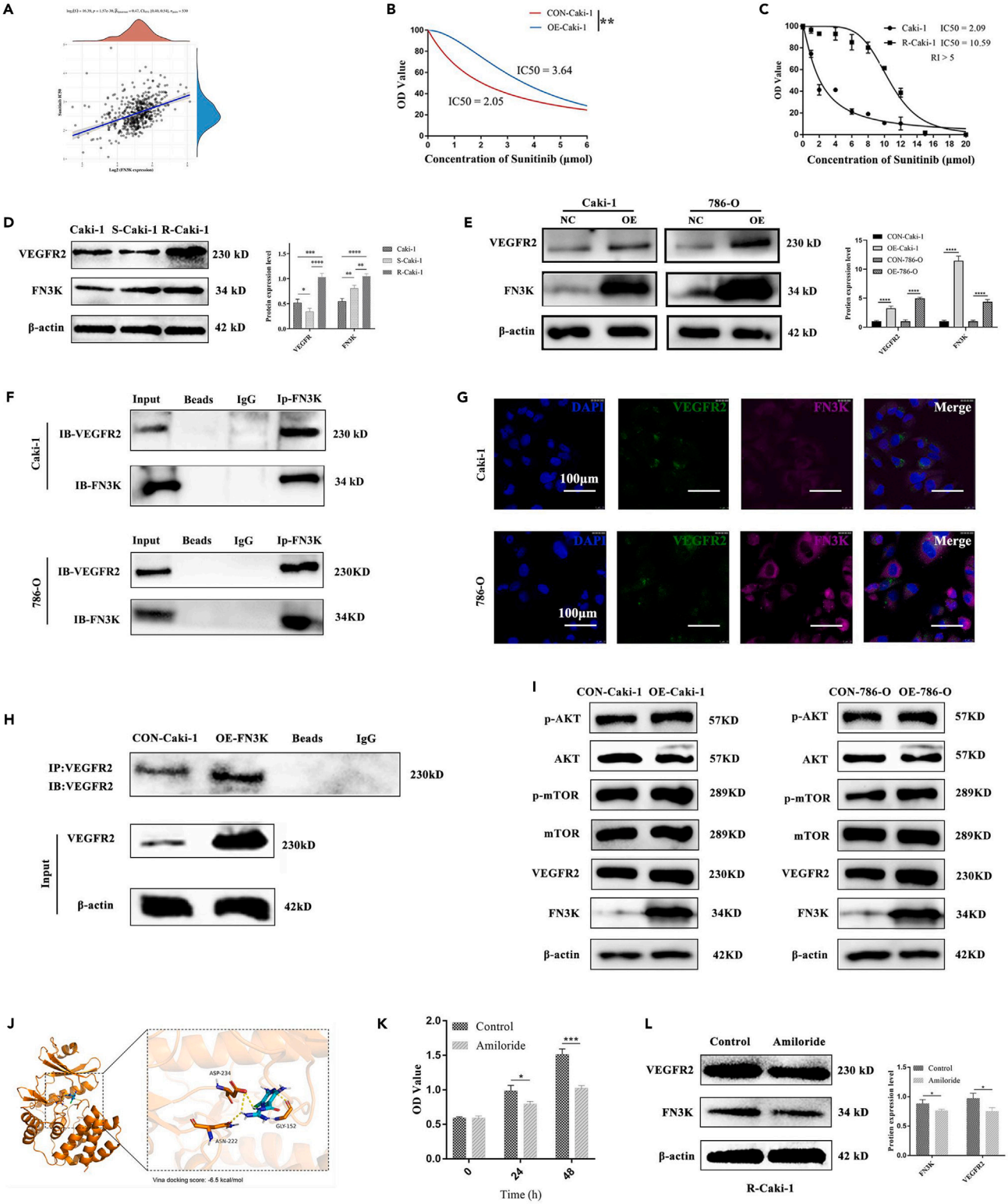

Figure 3. Amiloride down-regulated VEGFR2 via FN3K to restore the sensitivity of RCC to sunitinib

(A) Correlation between the expression of FN3K and the IC50 value of sunitinib in RCC.

(B) Drug sensitivity test to analyze the effect of the overexpression of FN3K on the IC50 value of sunitinib in Caki-1 cells.

(C) Construction of Caki-1 cell line resistant to sunitinib.

Figure 3. *Continued*

(D) WB to detect the expression of FN3K and VEGFR2 in Caki-1 cells, S-Caki-1 cells (sunitinib treated Caki-1 cells for 48 h) and R-Caki-1 cells.

(E) The expression of VEGFR2 was detected through WB subsequent to the overexpression of FN3K in Caki-1 and 786-O cells.

(F) Co-Immunoprecipitation analysis of FN3K and VEGFR2.

(G) IF to detect the binding condition of VEGFR2 (green) and FN3K (red).

(H) VEGFR2 was purified by immunoprecipitation, and the molecular weight of VEGFR2 in Caki-1 cells was detected by WB after FN3K overexpression.

(I) WB was used to show the FN3K, VEGFR2, mTOR, *p*-mTOR, AKT, P-AKT.

(J) AutoDock Vina 1.1.2 docking Analysis of Molecular docking between amiloride and FN3K.

(K) 6 μmol sunitinib continued to treat R-Caki-1 cells, followed by the addition of amiloride for a treatment of 48 h, CCK-8 reagent was used to detect cell activity.

(L) WB detected the expression of FN3K and VEGFR2 in R-Caki-1 cells treated with amiloride. *$p < 0.05$, **$p < 0.01$, ***$p < 0.001$, ****$p < 0.0001$.

DISCUSSION

Amiloride is a potassium-sparing diuretic that is frequently utilized in the clinical management of hypertension due to its mild nature.[14] Our findings indicated that amiloride could independently impede the proliferation of RCC and stimulate apoptosis in tumors, while also augmenting the antitumor efficacy of sunitinib. These results provided a promising outlook for the potential use of amiloride in combination therapy for cancer treatment. Here, we combined proteomics analysis and molecular biology techniques to demonstrate that amiloride enhances the response of RCC to sunitinib via FN3K.

Fructosamine-3-kinase (FN3K) is responsible for maintaining intracellular homeostasis, regulating signal transduction by inhibiting cellular activity such as oxidative stress and catalyzing the formation of fructosamine.[15–17] Serum fructosamine is a crucial factor in promoting the malignant transformation of normal cells,[18,19] indicating that FN3K may be implicated in the progression of tumorigenicity. A previous investigation indicated a decrease in the expression of FN3K in colon cancer compared to adjacent normal mucosa.[19] In contrast, another study showed that FN3K activated the carcinogenic Nrf2 by keeping it in a deglycated state, thus blocking FN3K activity benefited patients with hepatocellular carcinoma.[20] The above research indicated that FN3K played a complex and diverse role in cancer. Therefore, new therapeutic agents that regulate the activity of FN3K enzymes are essential for individual cancers by determining the specific role of FN3K in each type of cancer. Our study revealed that FN3K may serve as a carcinogenic factor in RCC by promoting its proliferation, invasion, and metastasis. It was found that FN3K can improve the prognosis of RCC through public database analysis, which was different from our results. The possible reason is that bioinformatics analysis can not accurately identify the actual situation of patients with tumor and further research is needed to clarify the biological significance of FN3K. On the other hand, the process of FN3K-mediated deglycation has been identified as a crucial mechanism for tumor cells to endure hypoxic conditions and develop drug resistance.[21] Notably, our findings indicated that FN3K could elevate the IC50 value of sunitinib in Caki-1 cells, corroborating with the outcomes of external database analysis. These results suggested that FN3K may significantly influence the sensitivity of RCC cells toward sunitinib.

Functional vascular networks are accountable for providing the majority of nutrients and oxygen required by solid tumors, and angiogenesis is a crucial factor in tumor progression and metastasis.[22,23] The VEGF-VEGFR pathway is a significant mechanism for regulating tumor neovascularization.[24] VEGFR2, the primary functional receptor of VEGF, governs the response of nearly all recognized cells to VEGF and is instrumental in promoting the proliferation and migration of vascular endothelial cells.[25,26] Consequently, it has emerged as one of the most efficacious targets for anti-tumor therapy. Sunitinib is a tyrosine kinase inhibitor (TKI) targeting VEGFR2, which exerts its apoptosis effect by inhibiting VEGFR2/Akt/mTOR signal pathway.[27,28] Continuous treatment of sunitinib induces tumor hypoxia and reactivates the angiogenic pathway of VEGF-VEGFR, making patients resistant to sunitinib.[29,30] Importantly, the activation of AKT/mTOR signal transduction helps to reduce the sensitivity of sunitinib in RCC.[31] We observed that the phosphorylation level of AKT/mTOR signal pathway increased with the increase of VEGFR2 expression in RCC cells overexpressed FN3K compared with the control group, suggesting FN3K may decrease the sensitivity of RCC to sunitinib through VEGFR2/AKT/mTOR signal pathway.

In our research, it is interesting that both *in vitro* and *in vivo* treatment of sunitinib enhanced the FN3K expression but declined the tumor volume and cancer cell proliferation respectively in RCC cell models. This study is also in line with study observed at *in vitro* levels for FN3K expression in breast carcinoma models treated by TKI.[32] At the same time, low-dose FN3K inhibitor oxaliplatin can enhance the effect of chemotherapy on breast cancer.[33] Therefore, we speculate that amiloride increases the sensitivity of RCC to sunitinib by reducing the expression of FN3K. Our study further demonstrated an upregulation of VEGFR2 and FN3K in R-Caki-1 cells. Importantly, the addition of amiloride effectively mitigated this phenomenon. Recent research has demonstrated that post-transcriptional glycation modified the function of VEGFR2, leading to aberrant downstream signal pathway transduction,[34] which is a crucial contributor in tumor angiogenesis, metastasis, and drug resistance.[35–37] The present findings revealed a protein interaction between FN3K and VEGFR2 and FN3K influenced the molecular weight alteration of VEGFR2. It is postulated that FN3K may act as a deglycating enzyme, promoting the deglycation of VEGFR2 and inducing RCC cells to develop resistance to sunitinib. Our work emphasized that the amiloride treatment of RCC may resensitize FN3K-induced sunitinib resistance. Collectively, this study provided a practical basis for further clinical application.

The findings of this investigation hold considerable importance for the clinical management of sunitinib sensitivity in patients with RCC. FN3K may bind VEGFR2 and exert deglycated function, regulate the biological process of VEGFR2, and activate AKT/mTOR pathway signaling. FN3K depletion mediated VEGFR2 disruption promotes amiloride synergized the anti-RCC activity of sunitinib. The down-regulation of FN3K by amiloride may represent a viable strategy for enhancing the clinical response to sunitinib in RCC. Furthermore, As a promising novel target for tumors, FN3K may play an important role in the progression and treatment of RCC.

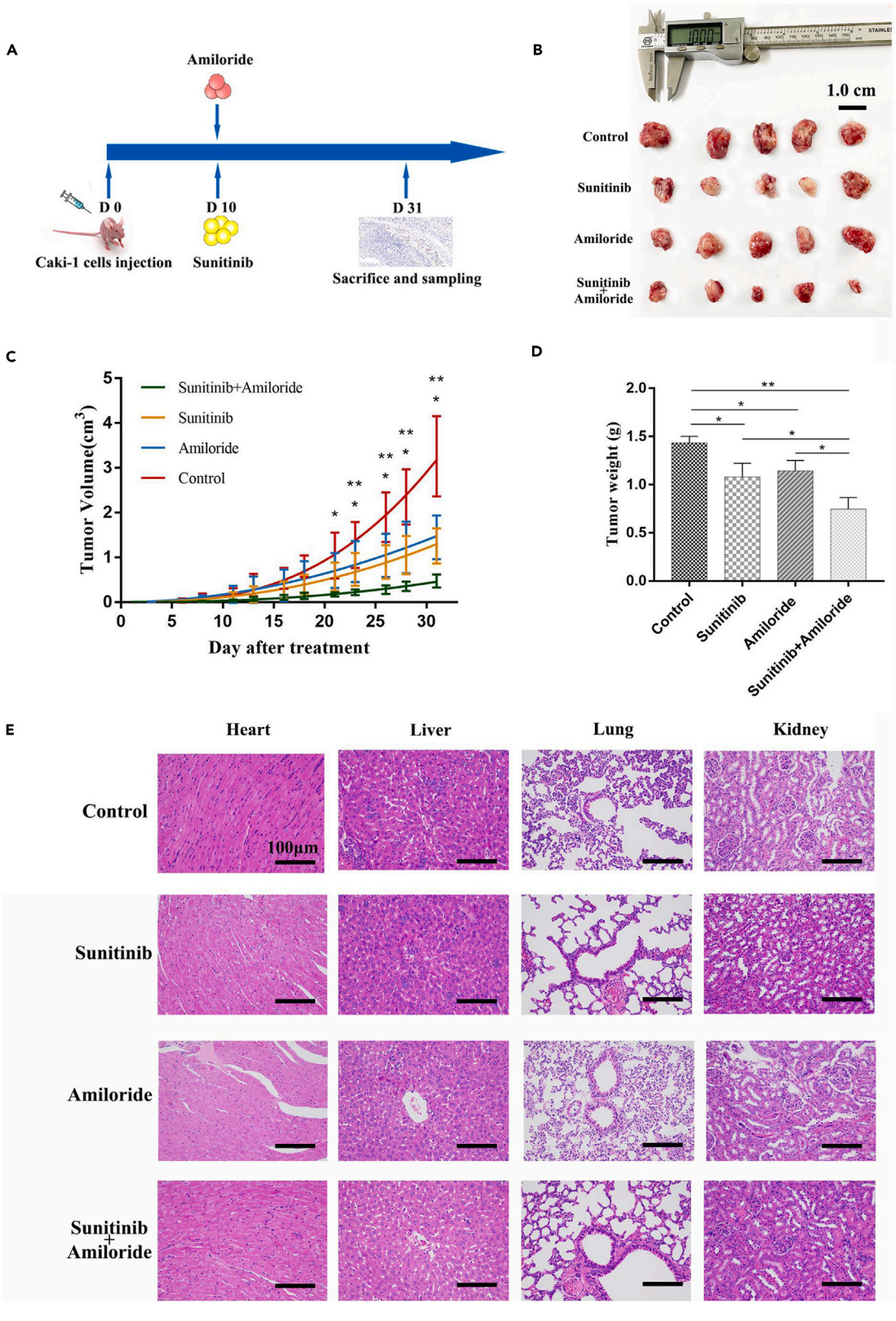
A
Amiloride
D 0
D 10
D 31
Caki-1 cells injection
Sunitinib
Sacrifice and sampling
B
1.0 cm
Control
Sunitinib
Amiloride
Sunitinib
+
Amiloride
C
Sunitinib+Amiloride
Sunitinib
Amiloride
Control
Tumor Volume(cm3)
Day after treatment
D
Tumor weight (g)
Control
Sunitinib
Amiloride
Sunitinib+Amiloride
E
Heart
Liver
Lung
Kidney
Control
100μm
Sunitinib
Amiloride
Sunitinib
+
Amiloride

Figure 4. The administration of amiloride enhanced the responsiveness of the Xenograft Model of RCC to sunitinib

(A) A cohort of BALB-c/Null mice bearing tumor were treated with 25 mg/kg sunitinib, 10 mg/kg amiloride and a combination of both drugs for 20 days, $N = 5$/group.

(B) Gross view of tumor.

(C) Growth curve of tumor volume. *$p < 0.05$, sunitinib with amiloride vs. control; **$p < 0.05$, sunitinib with amiloride vs. sunitinib or amiloride.

(D) The weight of tumors in each group.

(E) HE staining of heart, liver, lung and kidney in mice. *$p < 0.05$, **$p < 0.01$.

Limitations of the study

Despite the progress made in our study, there are still certain limitations that need to be acknowledged. Specifically, our observations were limited to the molecular interaction between FN3K and VEGFR2, and although FN3K could manipulate the molecular weight of VEGFR2, we could not definitively confirm VEGFR2 was deglycated.

STAR★METHODS

Detailed methods are provided in the online version of this paper and include the following:

- KEY RESOURCES TABLE
- RESOURCE AVAILABILITY
  - Lead contact
  - Materials availability
  - Data and code availability
- EXPERIMENTAL MODEL AND STUDY PARTICIPANT DETAILS

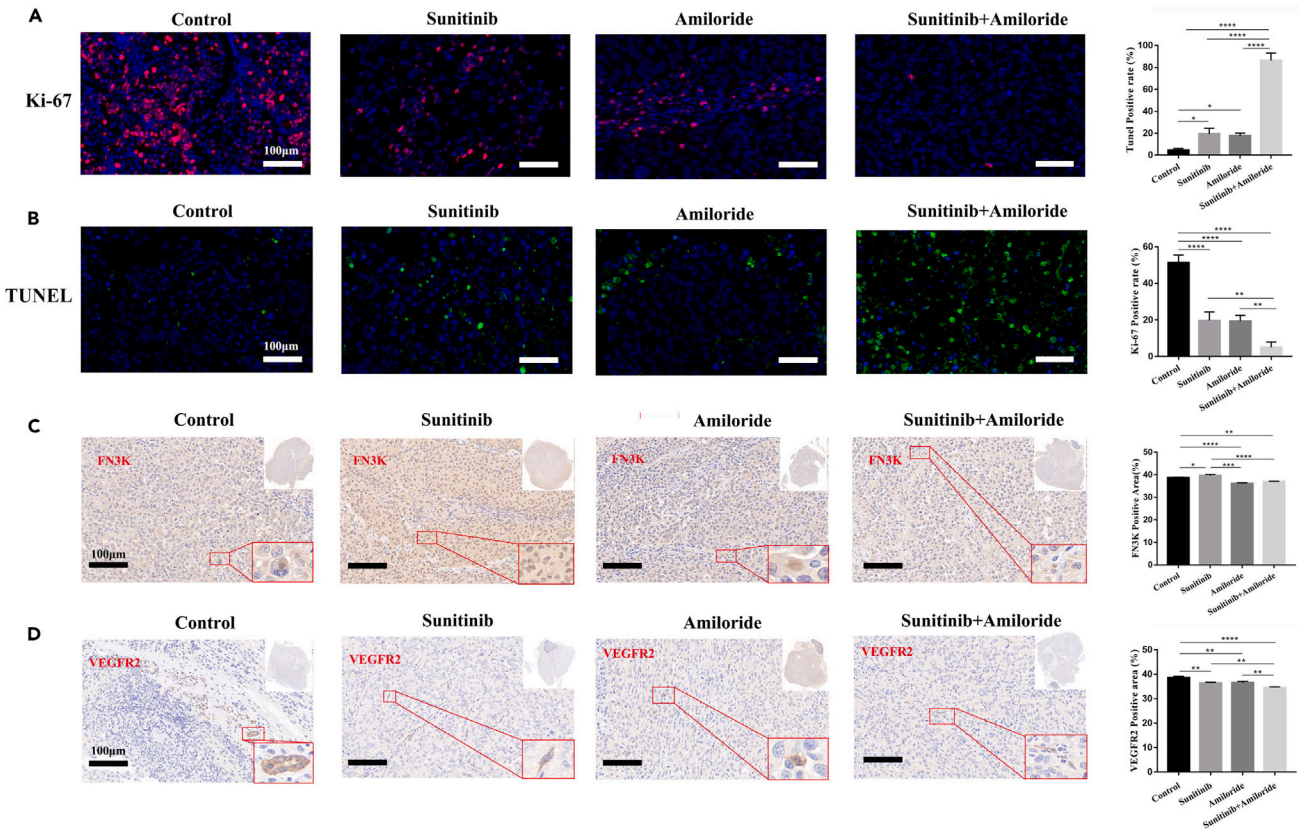

Figure 5. Effects of various drug treatments (25 mg/kg sunitinib, 10 mg/kg amiloride and their combination) on proliferation and apoptosis rate and expression of FN3K and VEGFR2 in Xenograft Model of RCC

(A) Representative images of Ki-67 IF staining in tumor tissue, Ki-67 positive cells (red).

(B) Representative images of TUNEL IF staining in tumor tissue, DNA leakages (green).

(C and D) Representative IHC images of FN3K and VEGFR2 in tumor tissue. *$p < 0.05$, **$p < 0.01$, ***$p < 0.001$, ****$p < 0.0001$.

SUPPLEMENTAL INFORMATION

Supplemental information can be found online at https://doi.org/10.1016/j.isci.2024.109997.

ACKNOWLEDGMENTS

This study was supported by the Natural Science Foundation of Fujian Province, China (No. 2019J01590) supports the study.

AUTHOR CONTRIBUTIONS

All authors read and approved the final article. Yuanyuan Bai and Yiqing You performed the experiments and wrote the article, Yingming Sun analyzed the data, Lixian Wu and Yongyang Wu designed the experiments. Daoxun Chen, Yongmei Chen, Zhenjie Yin, Shangfan Liao, Bingyong You, and Dongming Lu reviewed and revised the article.

DECLARATION OF INTERESTS

The authors declare no competing interests.

Received: October 9, 2023
Revised: April 10, 2024
Accepted: May 14, 2024
Published: May 16, 2024

REFERENCES

1. Cohen, H.T., and McGovern, F.J. (2005). Renal-cell carcinoma. N. Engl. J. Med. *353*, 2477–2490. https://doi.org/10.1056/NEJMra043172.
2. Capitanio, U., Bensalah, K., Bex, A., Boorjian, S.A., Bray, F., Coleman, J., Gore, J.L., Sun, M., Wood, C., and Russo, P. (2019). Epidemiology of Renal Cell Carcinoma. Eur. Urol. *75*, 74–84. https://doi.org/10.1016/j.eururo.2018.08.036.
3. Faivre, S., Demetri, G., Sargent, W., and Raymond, E. (2007). Molecular basis for sunitinib efficacy and future clinical development. Nat. Rev. Drug Discov. *6*, 734–745. https://doi.org/10.1038/nrd2380.
4. Rizzo, M., and Porta, C. (2017). Sunitinib in the treatment of renal cell carcinoma: an update on recent evidence. Ther. Adv. Urol. *9*, 195–207. https://doi.org/10.1177/1756287217713902.
5. Schmid, T.A., and Gore, M.E. (2016). Sunitinib in the treatment of metastatic renal cell carcinoma. Ther. Adv. Urol. *8*, 348–371. https://doi.org/10.1177/1756287216663979.
6. Jin, J., Xie, Y., Zhang, J.S., Wang, J.Q., Dai, S.J., He, W.F., Li, S.Y., Ashby, C.R., Jr., Chen, Z.S., and He, Q. (2023). Sunitinib resistance in renal cell carcinoma: From molecular mechanisms to predictive biomarkers. Drug Resist. Updat. *67*, 100929. https://doi.org/10.1016/j.drup.2023.100929.
7. Liao, S., Huang, H., Zhang, F., Lu, D., Ye, S., Zheng, L., Sun, Y., and Wu, Y. (2020). Differential expression of epithelial sodium channels in human RCC associated with the prognosis and tumor stage: Evidence from integrate analysis. J. Cancer *11*, 7348–7356. https://doi.org/10.7150/jca.48970.
8. Liu, C., Zhu, L.L., Xu, S.G., Ji, H.L., and Li, X.M. (2016). ENaC/DEG in Tumor Development and Progression. J. Cancer *7*, 1888–1891. https://doi.org/10.7150/jca.15693.
9. Jankun, J., Keck, R.W., Skrzypczak-Jankun, E., and Swiercz, R. (1997). Inhibitors of urokinase reduce size of prostate cancer xenografts in severe combined immunodeficient mice. Cancer Res. *57*, 559–563.
10. Sparks, R.L., Pool, T.B., Smith, N.K., and Cameron, I.L. (1983). Effects of amiloride on tumor growth and intracellular element content of tumor cells in vivo. Cancer Res. *43*, 73–77.
11. Evans, D.M., and Sloan-Stakleff, K. (2000). Suppression of the invasive capacity of human breast cancer cells by inhibition of urokinase plasminogen activator via amiloride and B428. Am. Surg. *66*, 460–464.
12. Alliegro, M.C., Alliegro, M.A., Cragoe, E.J., Jr., and Glaser, B.M. (1993). Amiloride inhibition of angiogenesis in vitro. J. Exp. Zool. *267*, 245–252. https://doi.org/10.1002/jez.1402670302.
13. He, B., Deng, C., Zhang, M., Zou, D., and Xu, M. (2007). Reduction of intracellular pH inhibits the expression of VEGF in K562 cells after targeted inhibition of the Na+/H+

exchanger. Leuk. Res. *31*, 507–514. https://doi.org/10.1016/j.leukres.2006.06.015.
14. Sun, Q., and Sever, P. (2020). Amiloride: A review. J. Renin. Angiotensin. Aldosterone. Syst. *21*, 1470320320975893. https://doi.org/10.1177/1470320320975893.
15. Delplanque, J., Delpierre, G., Opperdoes, F.R., and Van Schaftingen, E. (2004). Tissue distribution and evolution of fructosamine 3-kinase and fructosamine 3-kinase-related protein. J. Biol. Chem. *279*, 46606–46613. https://doi.org/10.1074/jbc.M407678200.
16. Kameya, M., Sakaguchi-Mikami, A., Ferri, S., Tsugawa, W., and Sode, K. (2015). Advancing the development of glycated protein biosensing technology: next-generation sensing molecules. J. Diabetes Sci. Technol. *9*, 183–191. https://doi.org/10.1177/1932296814565784.
17. Delpierre, G., Rider, M.H., Collard, F., Stroobant, V., Vanstapel, F., Santos, H., and Van Schaftingen, E. (2000). Identification, cloning, and heterologous expression of a mammalian fructosamine-3-kinase. Diabetes *49*, 1627–1634. https://doi.org/10.2337/diabetes.49.10.1627.
18. Misciagna, G., De Michele, G., Guerra, V., Cisternino, A.M., Di Leo, A., and Freudenheim, J.L.; INTEROSP Group (2004). Serum fructosamine and colorectal adenomas. Eur. J. Epidemiol. *19*, 425–432. https://doi.org/10.1023/b:ejep.0000027359.95727.24.
19. Notarnicola, M., Caruso, M.G., Tutino, V., Guerra, V., Frisullo, S., Altomare, D.F., and Misciagna, G. (2010). Reduced fructosamine-3-kinase activity and its mRNA in human distal colorectal carcinoma. Genes Nutr. *5*, 257–262. https://doi.org/10.1007/s12263-009-0165-y.
20. Sanghvi, V.R., Leibold, J., Mina, M., Mohan, P., Berishaj, M., Li, Z., Miele, M.M., Lailler, N., Zhao, C., de Stanchina, E., et al. (2019). The Oncogenic Action of NRF2 Depends on De-glycation by Fructosamine-3-Kinase. Cell *178*, 807–819.e21. https://doi.org/10.1016/j.cell.2019.07.031.
21. Ji, L., Li, H., Gao, P., Shang, G., Zhang, D.D., Zhang, N., and Jiang, T. (2013). Nrf2 pathway regulates multidrug-resistance-associated protein 1 in small cell lung cancer. PLoS One *8*, e63404. https://doi.org/10.1371/journal.pone.0063404.
22. Brown, J.M., and Giaccia, A.J. (1998). The unique physiology of solid tumors: opportunities (and problems) for cancer therapy. Cancer Res. *58*, 1408–1416.
23. Traxler, P. (2003). Tyrosine kinases as targets in cancer therapy - successes and failures. Expert Opin. Ther. Targets *7*, 215–234. https://doi.org/10.1517/14728222.7.2.215.
24. Folkman, J. (2006). Angiogenesis. Annu. Rev. Med. *57*, 1–18. https://doi.org/10.1146/annurev.med.57.121304.131306.
25. Musumeci, F., Radi, M., Brullo, C., and Schenone, S. (2012). Vascular endothelial growth factor (VEGF) receptors: drugs and new inhibitors. J. Med. Chem. *55*, 10797–10822. https://doi.org/10.1021/jm301085w.
26. Bold, G., Schnell, C., Furet, P., McSheehy, P., Brüggen, J., Mestan, J., Manley, P.W., Drückes, P., Burglin, M., Dürler, U., et al. (2016). A Novel Potent Oral Series of VEGFR2 Inhibitors Abrogate Tumor Growth by Inhibiting Angiogenesis. J. Med. Chem. *59*, 132–146. https://doi.org/10.1021/acs.jmedchem.5b01582.
27. Morais, C. (2014). Sunitinib resistance in renal cell carcinoma. J. Kidney Cancer VHL *1*, 1–11. https://doi.org/10.15586/jkcvhl.2014.7.
28. Saito, Y., Tanaka, Y., Aita, Y., Ishii, K.A., Ikeda, T., Isobe, K., Kawakami, Y., Shimano, H., Hara, H., and Takekoshi, K. (2012). Sunitinib induces apoptosis in pheochromocytoma tumor cells by inhibiting VEGFR2/Akt/mTOR/S6K1 pathways through modulation of Bcl-2 and BAD. Am. J. Physiol. Endocrinol. Metab. *302*, E615–E625. https://doi.org/10.1152/ajpendo.00035.2011.
29. Joosten, S.C., Hamming, L., Soetekouw, P.M., Aarts, M.J., Veeck, J., van Engeland, M., and Tjan-Heijnen, V.C. (2015). Resistance to sunitinib in renal cell carcinoma: From molecular mechanisms to predictive markers and future perspectives. Biochim. Biophys. Acta *1855*, 1–16. https://doi.org/10.1016/j.bbcan.2014.11.002.
30. Bhatt, R.S., Wang, X., Zhang, L., Collins, M.P., Signoretti, S., Alsop, D.C., Goldberg, S.N., Atkins, M.B., and Mier, J.W. (2010). Renal cancer resistance to antiangiogenic therapy is delayed by restoration of angiostatic signaling. Mol. Cancer Ther. *9*, 2793–2802. https://doi.org/10.1158/1535-7163.Mct-10-0477.
31. Sun, Y., Zhu, L., Liu, P., Zhang, H., Guo, F., and Jin, X. (2023). ZDHHC2-Mediated AGK Palmitoylation Activates AKT-mTOR Signaling to Reduce Sunitinib Sensitivity in Renal Cell Carcinoma. Cancer Res. *83*, 2034–2051. https://doi.org/10.1158/0008-5472.Can-22-3105.
32. Beeraka, N.M., Zhang, J., Mandal, S., Vikram P R, H., Liu, J., BM, N., Zhao, D., Vishwanath, P., B, M.G., and Fan, R. (2023). Screening fructosamine-3-kinase (FN3K) inhibitors, a deglycating enzyme of oncogenic Nrf2: Human FN3K homology modelling, docking and molecular dynamics simulations. PLoS One *18*, e0283705. https://doi.org/10.1371/journal.pone.0283705.
33. Beeraka, N.M., Zhang, J., Zhao, D., Liu, J., A, U.C., Vikram Pr, H., Shivaprakash, P., Bannimath, N., Manogaran, P., Sinelnikov, M.Y., et al. (2023). Combinatorial Implications of Nrf2 Inhibitors with FN3K Inhibitor: In vitro Breast Cancer Study. Curr. Pharm. Des. *29*, 2408–2425. https://doi.org/10.2174/0113816128261466231011114600.
34. Rahimi, N., and Costello, C.E. (2015). Emerging roles of post-translational modifications in signal transduction and angiogenesis. Proteomics *15*, 300–309. https://doi.org/10.1002/pmic.201400183.
35. Croci, D.O., Cerliani, J.P., Dalotto-Moreno, T., Méndez-Huergo, S.P., Mascanfroni, I.D., Dergan-Dylon, S., Toscano, M.A., Caramelo, J.J., García-Vallejo, J.J., Ouyang, J., et al. (2014). Glycosylation-dependent lectin-receptor interactions preserve angiogenesis in anti-VEGF refractory tumors. Cell *156*, 744–758. https://doi.org/10.1016/j.cell.2014.01.043.
36. Fukushima, R., Kasamatsu, A., Nakashima, D., Higo, M., Fushimi, K., Kasama, H., Endo-Sakamoto, Y., Shiiba, M., Tanzawa, H., and Uzawa, K. (2018). Overexpression of Translocation Associated Membrane Protein 2 Leading to Cancer-Associated Matrix Metalloproteinase Activation as a Putative Metastatic Factor for Human Oral Cancer. J. Cancer *9*, 3326–3333. https://doi.org/10.7150/jca.25666.
37. Nagy, J.A., Chang, S.H., Dvorak, A.M., and Dvorak, H.F. (2009). Why are tumour blood vessels abnormal and why is it important to know? Br. J. Cancer *100*, 865–869. https://doi.org/10.1038/sj.bjc.6604929.
38. Rozanova, S., Barkovits, K., Nikolov, M., Schmidt, C., Urlaub, H., and Marcus, K. (2021). Quantitative Mass Spectrometry-Based Proteomics: An Overview. Methods Mol. Biol. *2228*, 85–116. https://doi.org/10.1007/978-1-0716-1024-4_8.

STAR★METHODS

KEY RESOURCES TABLE

REAGENT or RESOURCE	SOURCE	IDENTIFIER
Antibodies		
Bax (E4U1V) Rabbit mAb	Cell Signaling Technology	Cat# 41162; RRID:AB_2924730
Bcl-2 (124) Mouse mAb	Cell Signaling Technology	Cat# 15071; RRID:AB_2744528
Anti-FN3K antibody	Abcam	RRID: ab228639;
FN3K Polyclonal antibody	Proteintech	RRID: 14293-1-AP
VEGF Receptor 2 (D5B1) Rabbit mAb	Cell Signaling Technology	Cat# 9698; RRID:AB_11178792
VEGFR2/KDR Polyclonal antibody	Proteintech	RRID: 26415-1-AP
Cy3 conjugated Goat Anti-mouseIgG(H+L) GB21301	Servicebio	RRID: GB21301
FITC conjugated Goat Anti-Mouse IgG (H+L)	Servicebio	RRID: GB22301
AKT Monoclonal antibody	Proteintech	RRID: 60203-2-Ig
Phospho-AKT (Ser473) Recombinant antibody	Proteintech	RRID: 80455-1-RR
mTOR Monoclonal antibody	Proteintech	RRID: 66888-1-Ig
Phospho-mTOR (Ser2448) Monoclonal antibody	Proteintech	RRID: 67778-1-Ig
β-Actin (13E5) Rabbit mAb	Cell Signaling Technology	Cat#4970S; RRID:AB_2223172
GAPDH (D16H11) XP® Rabbit mAb (BSA and Azide Free)	Cell Signaling Technology	RRID: 92310
HRP-conjugated secondary rabbit antibody	EpiZyme	RRID: LF102
HRP-conjugated secondary mouse antibody	EpiZyme	RRID: LF103
Bacterial and virus strains		
pcSLenti-EF1-EGFP-P2A-BSR-CMV-FN3K-3xFLAG-WPRE	Obio Technology Corp (Shanghai, China)	https://www.obio-tech.com/
pcSLenti-EF1-EGFP-P2A-BSR-CMV-MCS-WPRE	Obio Technology Corp (Shanghai, China)	https://www.obio-tech.com/
Chemicals, peptides, and recombinant proteins		
Sunitinib	MedChemExpress	RRID: HY-10255A
Amiloride hydrochloride	MedChemExpress	RRID: HY-B0285A
Protein A/G Magnetic Beads	MedChemExpress	RRID: HY-K0202
Crystal violet	Solarbio	RRID: G1063
Puromycin	Sigma	RRID: 540411
Matrix gel	Corning	N/A
Critical commercial assays		
Cell Counting Kit-8	MCE	RRID: HY-K0301
Annexin V-FITC/PI Apoptosis Kit	MultiSciences	RRID: AT101
Column Tissue & Cell Protein Extraction Kit	Epizyme	RRID: PC201PLUS
Deposited data		
RNA-seq data	TCGA	portal.gdc.cancer.gov/
Proteomics data	iproX database	IPX0008759000
Experimental models: Cell lines		
Caki-1	Chinese Academy of Sciences	Cat# TCHu135; RRID:CVCL_0234
786-O	Chinese Academy of Sciences	Cat# TCHu186; RRID:CVCL_1051
Experimental models: Organisms/strains		
BALB/c-Nu	SLAC ANIMAL	N/A

(*Continued on next page*)

Continued

REAGENT or RESOURCE	SOURCE	IDENTIFIER
Software and algorithms		
R version 4.3.1	The R Foundation	https://www.r-project.org/
CompuSyn	CompuSyn Inc.	www.combosyn.com
ImageJ	National Institutes of Health	https://imagej.net/ij/index.html
GraphPad Prism 8.0 Software	GraphPad Inc.	https://www.graphpad.com
FlowJo	FlowJo	https://www.flowjo.com/

RESOURCE AVAILABILITY

Lead contact

Further information and requests for resources and reagents should be directed to and will be fulfilled by the lead contact, Yongyang Wu (wuyyfj@fjmu.edu.cn).

Materials availability

This study did not generate new unique reagents.

Data and code availability

- The RNA-seq data have been deposited at TCGA datebase and is publicly available (https://portal.gdc.cancer.gov/). The proteomics data have been deposited to the ProteomeXchange Consortium via the iProX repository with the dataset identifier IPX0008759000 (https://www.iprox.cn/page/home.html).
- This article contains no original code.
- Any additional information required to reanalyze the data reported in this paper is available from the lead contact upon request.

EXPERIMENTAL MODEL AND STUDY PARTICIPANT DETAILS

Cell lines

Caki-1 and 786-O cells were purchased from Type Culture Bank (Chinese Academy of Sciences, Shanghai, China) and validated by short, repeated sequencing (Cellcook Biotech, Guangzhou, China). Cells were cultured in RPMI-1640 medium (HyClone, USA) containing 10% fetal bovine serum (Gibco, Cat) and cultured at 37°C in a 5% CO_2 atmosphere.

Animals

6-8 week-old BALB/C female nude mice were purchased from Shanghai Slaughter Laboratory Animal Co. Animal experiments were approved by the Animal Ethics Committee of Fujian Medical University. All animals were housed for one week before the experiments in light/dark cycles (12 h light:12 h dark, LD), constant temperature (23±2°C), constant humidity (50±5%), 6 animals per cage, and free access to water and diet. Approximately 5×10^6 Caki-1 cells were collected, resuspended in 100 μl PBS, and injected into the right subcutis of each mouse. Treatment was initiated when the tumor size reached approximately 100 mm^3. 25mg/kg sunitinib, 10mg/kg amiloride and their combination were intragastriced once a day. The tumor size and body weight of mice were recorded daily. After 33 days of treatment, mice were sacrificed, and tumor size was assessed. Tumor volume (V) was calculated by the formula $\pi/6 \times \text{length} \times \text{width}^2$.

METHOD DETAILS

Cell viability assay

Cell viability was determined using the CCK-8 assay. Cells were seeded in 96-well plates at 3,000-5,000 cells/well density and incubated for 24h. They were then exposed to different concentrations of sunitinib, 0.15mmol/L amilorid and their combinations for 48h. Non-linear regression using GraphPadPrism 8.0 was performed to calculate the value of the semi-inhibitory concentration of 50% reduction in proliferation compared to the untreated control group. Synergistic analysis of the combined effect of sunitinib and amiloride was performed using CompuSyn software. Combination Index (CI) values lower than 1.0 were considered synergistic. Cell proliferation inhibition rate (%) = (OD Value of experimental group - OD Value of blank control group) / (OD Value of control group - OD Value of blank control hole OD450) × 100%. Subsequently, Q value as the following: $Q = E_{(A+B)}/[E_A + E_B\text{-}E_A \times E_B]$, $E_A + E_B$ is the inhibition rate of combination treatment, E_A and E_B are the inhibition rate of single treatment. The effect of combination treatment is considered synergism ($Q > 1.15$), additive effect ($0.85 < Q < 1.15$), or antagonism ($Q < 0.85$).

Colony formation assay

Cells were placed on 6-well plates (100-200 cells/well) containing 2mL of complete medium, incubated for 24h, and then treated with 0.5% DMSO, 2μmol/L sunitinib, 0.15mmol/L amiloride and their combinations for 10-15d. Colonies were fixed with 4% paraformaldehyde (PFA) and stained with crystal violet. These cells were photographed, and the number of colonies was counted.

Flow cytometry

Cells in the logarithmic growth phase were seeded in 6-well plates, control and experimental groups were set up. After the cells plastered, the cells were treated with a medium containing 2μmol/L sunitinib, 0.15mmol/L amiloride and the combination of the two drugs and incubated continuously in a CO_2 incubator for 48h. 500μL binding buffer to resuspend the cells, add 5μL annexinV-FITC and 10μl propidium iodide mix well at room temperature and avoid light for 15min. The stained cells were assessed by flow cytometry.

Quantitative proteomics

Caki cells were treated with amiloride (0.15mmol/L) or/and sunitinib (2μmol/L) for 48h. After obtaining the annotation information of all the proteins in each group identified by mass spectrometry, the relevant information of the differentially expressed proteins was extracted, the categories and numbers were counted, and a hypergeometric test performed the functional enrichment analysis. The significant functional categories relevant to this experiment could be screened.[38]

Transfection of lentivirus

FN3K overexpression lentivirus were designed by Obio Technology Corp. Then, Caki-1 cells were transfected with the lentivirus, according to the manufacturer's instructions. Stable cell lines were screened with 10μg/mL puromycin for 1 week. Overexpression efficiencies of FN3K were assessed by Western blot.

CCK-8

Cell proliferation assays were performed by seeding 1000 cells in 96-well plates and incubating for 24, 48, 72, and 96h. 10μl CCK-8 was added to each well and incubated for 2h at 37°C. The absorbance at 450nm was measured with a Rayto-6000 system and normalized to RPMI-1640 medium as a control.

Transwell chamber

Cells were seeded into the upper chambers of 12-well plates (1×10^5 cells/well) and incubated for 24h. Transwell membranes were pre-coated with matrix gel for invasion assays at 37°C. After 24h, cells were fixed with 4% PFA and stained with 0.1% crystalline violet. Invading and migrating cells were counted under a phase contrast microscope (Leica, Germany) in 5 random fields per chamber.

Wound healing

Caki-1 cells seeded in 6-well plates were scratched, washed with PBS supplemented with 1% fetal bovine serum, and treated as indicated 24h later, several pre-labeled spots of the cells were photographed with a phase-contrast microscope. Migration rate was calculated as the ratio of the initial scratch distance for each sample to the average distance between the two sides of the free area of the cells.

Construct resistant cell lines

The caki-1 cell line was selected as the parental cell to establish a sunitinib-resistant cell line using the drug concentration increment method to induce drug resistance. The half inhibition rate IC50 of Caki-1 against sunitinib was determined, and a concentration similar to the IC50 was selected as the starting concentration for induction. The medium was changed periodically to remove the dead cells. The surviving cells grew slowly until they adapted to the drug concentration and grew to a whole bottle, and then the drug concentration was increased appropriately. So on and so forth, change the medium, pass on, increase the drug concentration until the drug resistance index of the resistant cell line and the parental cells to sunitinib > 5, can be considered as drug resistance, said the construction success, said "R-Caki-1".

Co-immunoprecipitation (Co-IP)

Cells were lysed with RIPA lysis buffer and prepared for Co-IP assay. After the Protein A/G Magnetic Beads were incubated with the primary antibody or IgG at 4°C for 4h, the prepared cell lysate was added to the mixture of beads and antibody overnight at 4°C. Then, the above mixture was washed with PBS containing 0.5% Tween-20 five times and eluted with SDS-PAGE sample loading buffer boiling for 5 min at 100°C, then analyzed by Western blot.

Western Blotting (WB)

Cultured cell lysates were prepared using a Column Tissue & Cell Protein Extraction Kit. Proteins were subjected to electrophoresis in 4–12% SDS-PAGE gel, shifted onto nitrocellulose membrane, followed by blocking with 5% non-fat milk and then incubated with corresponding primary antibodies including anti-Bax, anti-Bcl-2, anti-FN3K, anti-VEGFR2, anti-AKT, anti-p-AKT, anti-mTOR, anti-p-mTOR, anti-β-actin

and anti-GAPDH overnight at 4°C. Then membranes were incubated with HRP-conjugated secondary rabbit/mouse antibody for 1h. Finally, Omni-ECL chemiluminescent reagent was used to visualize the blots.

Immunohistochemical (IHC)

The tissues obtained from mice bearing tumors were fixed in 4% PFA at 4°C for an overnight period, followed by embedding in paraffin using a tissue processor. Subsequently, paraffin sections (5 μm) were obtained using a rotation microtome. The images were captured using Versa 8 (Leica, Germany), and the integrated optical density of IHC sections was determined using Image-Pro Plus 6.0.

Immunofluorescence (IF)

The Caki-1 cells obtained from Xenograft tumor models were cultured on 24-mm coverslips, fixed with 4% paraformaldehyde for 30 minutes, permeabilized with 0.1% Triton X-100, and blocked with 5% bovine serum albumin at room temperature for 1 hour. Following overnight incubation with primary antibodies at 4°C, the cells were exposed to Cy 3-labelled or FITC-labelled secondary antibodies at room temperature for 1h. Nuclei were stained with DAPI (2μg/ml). Immunofluorescent staining was visualized using either a fluorescent microscope (IX 73 DP80, Olympus, Japan) or a laser confocal microscope (Nikon, Japan). The mean density was utilized for semi-quantitative analysis.

Bioinformatics and drug sensitivity analysis

The analysis was performed using R (version 4.3.1). RNA-seq data were obtained from The Cancer Genome Atlas (TCGA) dataset for 881 RCC patients. For different FN3K expression groups, differential genes were identified and further enriched. Then, the prognostic significance and correlation of clinical features of FN3K were identified, and nomogram were constructed using univariate and multifactor COX analysis. Chemotherapy response was predicted for each sample based on the largest publicly available pharmacogenomics database, Genomics of Drug Sensitivity in Cancer (GDSC). The prediction process was implemented by the R package pRRophetic, in which the half-maximal inhibitory concentration (IC50) of samples was estimated by ridge regression, all parameters were set at default values, batch effects of combat and all tissue types were used, and duplicate gene expression was summarized as the mean.

QUANTIFICATION AND STATISTICAL ANALYSIS

Statistical analysis was performed using GraphPad Prism 8.0. The two groups were subjected to double-tailed unmatched students' t-test or paired t-test, as illustrated. For groups with non-normal distribution variables, Wilcoxon rank sum test was employed for statistical analysis. A significance level of $p<0.05$ was deemed statistically significant for all tests. Differences were considered statistically significant at the level of $p<0.05$ (*$p<0.05$, **$p<0.01$, ***$p<0.001$, ****$p<0.0001$), while all error bars represent mean ± standard deviation unless otherwise specified.